Methane Activation

Deutsche Ausgabe: DOI: 10.1002/ange.201600618
Internationale Ausgabe: DOI: 10.1002/anie.201600618

Activation of Methane Promoted by Adsorption of CO on $Mo_2C_2^-$ Cluster Anions

Qing-Yu Liu, Jia-Bi Ma, Zi-Yu Li, Chongyang Zhao, Chuan-Gang Ning, Hui Chen,* and Sheng-Gui He**

Abstract: *Atomic clusters are being actively studied for activation of methane, the most stable alkane molecule. While many cluster cations are very reactive with methane, the cluster anions are usually not very reactive, particularly for noble metal free anions. This study reports that the reactivity of molybdenum carbide cluster anions with methane can be much enhanced by adsorption of CO. The $Mo_2C_2^-$ is inert with CH_4 while the CO addition product $Mo_2C_3O^-$ brings about dehydrogenation of CH_4 under thermal collision conditions. The cluster structures and reactions are characterized by mass spectrometry, photoelectron spectroscopy, and quantum chemistry calculations, which demonstrate that the $Mo_2C_3O^-$ isomer with dissociated CO is reactive but the one with non-dissociated CO is unreactive. The enhancement of cluster reactivity promoted by CO adsorption in this study is compared with those of reported systems of a few carbonyl complexes.*

Methane, a ubiquitous raw material from fossil and biogenic sources, constitutes an important feedstock for the synthesis of value-added chemicals and one of the major energy sources.[1] Due to the high stability of methane C–H bonds, methane transformation is usually carried out under extreme conditions.[2] Furthermore, attempts aimed at uncovering the elementary steps and mechanisms associated with methane transformations have been proved particularly challenging.[1a,2a,3] Therefore, scientists have been striving for decades to articulate the fundamental principles of methane activation under mild conditions.[1b,4]

In the last decades, gas phase cluster species composed of limited numbers of atoms have been generally considered as ideal models for active sites of condensed phase systems.[5] The cluster studies have provided valuable mechanistic insights under thermal collision conditions. Three general mechanisms for methane activation can be classified: 1) activation by oxygen-centered radicals through hydrogen atom transfer (HAT),[5f,g] 2) activation by metal centers through oxidative addition (OA),[5e,6] and 3) ligand exchange through σ-bond metathesis ($ML + CH_4 \rightarrow MCH_3 + HL$).[7] Furthermore, most of the reactive species identified are cluster cations[5d–g] and the reactive anions usually contain noble metal elements such as Pt[8] and Ru.[9] For noble metal-free cluster anions, only lanthanum ($La_6O_{10}^-$ and $La_8O_{13}^-$)[10] and iron systems ($Fe(CO)_2^-$ and FeC_6^-)[11] have been reported to react with methane through the HAT and OA mechanisms, respectively. The reaction efficiencies of these noble metal-free anions are rather small ($\Phi = 0.02$–$0.04\,\%$). In the reactions of the iron species with CH_4, only the molecular addition products $Fe(CO)_2CH_4^-$ and $FeC_6CH_4^-$ were observed.[11] Herein, we report that dehydrogenation of methane by noble metal-free cluster anions ($Mo_2C_2^-$) can be promoted by adsorption of small molecules (CO) so that the reaction efficiency can be much enhanced ($\Phi = 0.8\,\%$).

Inspired by the evidence that molybdenum carbide clusters can activate CH_4 to form hydrogen and benzene on Mo/HZSM-5 catalysts,[3e,12] we generated $^{98}Mo_xC_y^-$ clusters and studied the reactions with CH_4 in an ion trap reactor under thermal collision conditions.[13] Our mass spectrometry (MS) measurements indicated that molybdenum carbide cluster anions $MoC_{1\text{-}6}^-$ and $Mo_2C_{2\text{-}7}^-$ were not reactive with CH_4 ($\Phi < 0.01\,\%$) (Figure S2 in the Supporting Information). For example, the mass spectrum shown in Figure 1 a1 indicates that $Mo_2C_2^-$ alone could not react with CH_4. Unexpectedly, with the presence of CO in the reactant gas (Figure 1 a2), the CO addition product $Mo_2C_3O^-$ could react with CH_4 to generate $Mo_2C_3OCH_2^-$:

$$Mo_2C_2^- + CO \rightarrow Mo_2C_3O^- \quad (1)$$

$$Mo_2C_3O^- + CH_4 \rightarrow Mo_2C_3OCH_2^- + H_2 \quad (2)$$

The $Mo_2C_3O^-$ anion could also be generated by seeding CO (Figure 1 b1) or O_2 (Figure 1 c1) in the cluster generation gas (see Experimental Section) and such formed $Mo_2C_3O^-$ is

[*] Q.-Y. Liu, Dr. Z.-Y. Li, Prof. Dr. S.-G. He
Beijing National Laboratory for Molecular Science, State Key Laboratory for Structural Chemistry of Unstable and Stable Species, Institute of Chemistry, Chinese Academy of Sciences
Beijing 100190 (China)
E-mail: shengguihe@iccas.ac.cn
Dr. J.-B. Ma
Key Laboratory of Cluster Science, Institute for Chemical Physics
School of Chemistry, Beijing Institute of Technology
Beijing 100081 (China)
E-mail: majiabi@bit.edu.cn
C. Zhao, Prof. Dr. H. Chen
Beijing National Laboratory for Molecular Science, Key Laboratory of Photochemistry, Institute of Chemistry, Chinese Academy of Sciences
Beijing 100190 (China)
E-mail: chenh@iccas.ac.cn
Prof. Dr. C.-G. Ning
Department of Physics, State Key Laboratory of Low-Dimensional Quantum Physics, Tsinghua University
Beijing 100084 (China)
Q.-Y. Liu, C. Zhao
University of Chinese Academy of Sciences
Beijing 100049 (China)

Supporting information for this article can be found under: http://dx.doi.org/10.1002/anie.201600618.

denoted as $(Mo_2C_3O^-)_{CO}$ or $(Mo_2C_3O^-)_{O2}$, respectively. The $(Mo_2C_3O^-)_{O2}$ species appeared to be more reactive than $(Mo_2C_3O^-)_{CO}$ in the reaction with CH_4, as can be seen from the relative intensities of the $Mo_2C_3OCH_2^-$ products in Figure 1 c2 versus 1 b2. In addition, the $(Mo_2C_3O^-)_{CO}$ could react with water impurity in the gas handling system during the process of confining and cooling the ions: $Mo_2C_3O^- + H_2O \rightarrow Mo_2C_2H_2O^- + CO$ (Figure 1 b1) while such an exchange reaction was barely observed for $(Mo_2C_3O^-)_{O2}$ (Figure 1 c1). Figures 1 c3 and S3 show the spectra with CD_4 and $^{13}CH_4$ isotopic compounds and the results confirm the dehydrogenation reaction (2). The $Mo_2C_4O_2^-$ and $Mo_2C_5O_3^-$ ions $[Mo_2C_2(CO)_{2,3}^-]$ were not reactive with CO (Figure S3). The $Mo_3C_{3\text{-}7}^-$ cluster ions were also generated and selected to react with CH_4 while only weak product signal of $Mo_3C_4CH_2^-$ was observed in $Mo_3C_4^- + CH_4$ (Figure S2). The enhanced reactivity of methane activation associated with adsorption of CO on $Mo_2C_2^-$ (Figure 1) is very interesting and is the focus of this study.

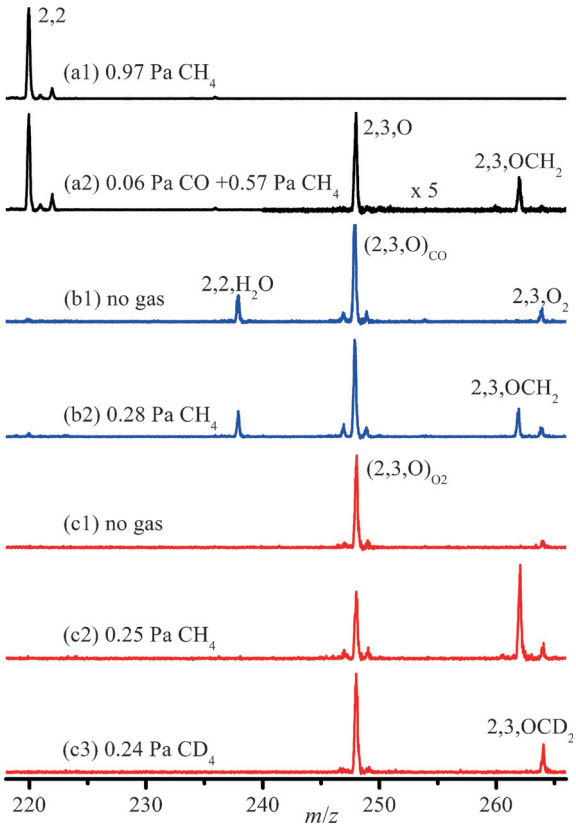

Figure 1. Cluster reactivity: Time-of-flight mass spectra for the reactions of mass-selected $^{98}Mo_2C_2^-$ (a), $(^{98}Mo_2C_3O^-)_{CO}$ (b), and $(^{98}Mo_2C_3O^-)_{O2}$ (c) with CH_4 (a1, b2, and c2), CD_4 (c3), and mixed CO and CH_4 (a2) for about 2.3 ms. The reactant gas pressures are shown. The $Mo_xC_yZ^-$ (Z = O, H_2O, etc.) species are labeled as *x*,*y*,Z.

The ion intensities of $(Mo_2C_3O^-)_X$ (I_R^X, in which X = CO or O_2) and the corresponding dehydrogenation products $(Mo_2C_3OCH_2^-)_X$ (I_P^X) at various CH_4 pressures (P) were recorded (Figure 2). The normalized intensities could be well fitted with the equations below:

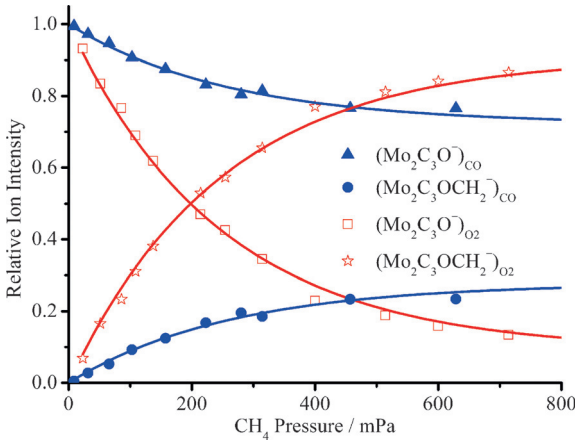

Figure 2. Reaction kinetics: Variations of the ion intensities with respect to CH_4 pressures in the reactivity experiments for $(Mo_2C_3O^-)_{CO}$ and $(Mo_2C_3O^-)_{O2}$.

$$I_R^X = (1 - a^X) + a^X \exp\left(-k_1^X \frac{P}{k_B T} t_R\right) \quad (3)$$

$$I_P^X = a^X \left[1 - \exp\left(-k_1^X \frac{P}{k_B T} t_R\right)\right] \quad (4)$$

in which α^X is the percentage of reactive component of $(Mo_2C_3O^-)_X$ with the pseudo-first-order rate constant of k_1^X, k_B is the Boltzmann constant, T is the temperature ($\approx$298 K), and t_R is the reaction time. The α^{CO} and α^{O2} were determined to be (28 ± 1)% and (91 ± 1)%, respectively. The k_1^{CO} and k_1^{O2} are close to each other: $(7.9 \pm 2.4) \times 10^{-12}$ and $(8.3 \pm 2.5) \times 10^{-12}$ cm^3 molecule^{-1} s^{-1}, corresponding to reaction efficiencies (Φ)[14] of 0.81% and 0.85%, respectively. The kinetic isotope effect $k_1[(Mo_2C_3O^-)_{O2} + CH_4]/k_1[(Mo_2C_3O^-)_{O2} + CD_4]$ was determined to be 7 ± 2.

The MS data suggest that both $(Mo_2C_3O^-)_{O2}$ and $(Mo_2C_3O^-)_{CO}$ have reactive and unreactive components (isomers). For the structures of $Mo_2C_3O^-$ (Figure 3), density functional theory (DFT) calculations determined two very stable isomers **2** and **3**, which are separated by a transition state with a high barrier (**4**/**3** in Figures 3 b and S7). The isomer **3** was predicted to be more stable than **2** by 0.51 eV. The experimentally generated $Mo_2C_3O^-$ can be the mixture of these two isomers. Because $(Mo_2C_3O^-)_{CO}$ was generated by seeding CO in the carrier gas, it is expected that isomer **2** with the un-broken C=O bond is relatively more abundant in $(Mo_2C_3O^-)_{CO}$ and less abundant in $(Mo_2C_3O^-)_{O2}$.

The photoelectron spectroscopy (PES) was used to further characterize the cluster structures. At 550 nm excitation (Figure 3 c), the photoelectron spectrum of $(Mo_2C_3O^-)_{CO}$ around 1.5 eV is relatively more intense than that of $(Mo_2C_3O^-)_{O2}$. In contrast, at 405 nm excitation (Figure 3 d), the photoelectron spectrum of $(Mo_2C_3O^-)_{CO}$ around 2.3 eV is relatively weaker than that of $(Mo_2C_3O^-)_{O2}$. The first photoelectron bands of **2** and **3** from the DFT-based Franck–Condon simulations are around 1.5 eV (Figure 3 c) and 2.3 eV (Figure 3 d), respectively, which interprets the PES results. In the MS experiments, the reactive component of $(Mo_2C_3O^-)_{O2}$ is more abundant (91% versus 28%) than that of

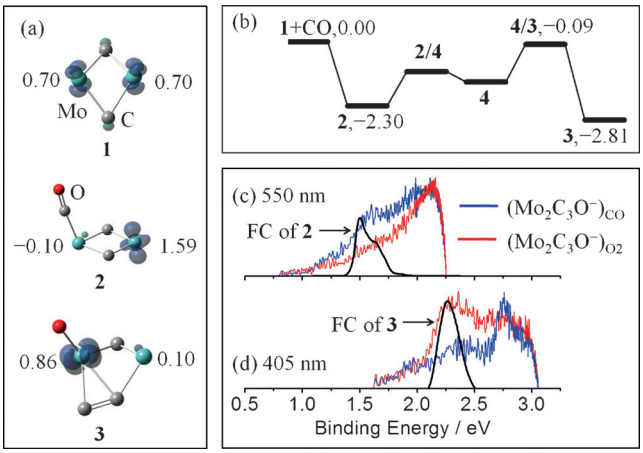

Figure 3. Structures and characterization: DFT calculated structures of $Mo_2C_2^-$ and $Mo_2C_3O^-$ (a) and potential energy profile for CO adsorption and dissociation on $Mo_2C_2^-$ (b) in doublet spin state; and photoelectron spectra of $(Mo_2C_3O^-)_{CO}$ and $(Mo_2C_3O^-)_{O2}$ taken with excitation laser wavelengths at 550 nm (c) and 405 nm (d). The spin density values (in μ_B) on Mo (a), relative energies (in eV) of **2** and **3** (b), and Franck–Condon (FC) simulations of the first photoelectron bands of **2** (c) and **3** (d) are shown. The spectra of $(Mo_2C_3O^-)_{CO}$ and $(Mo_2C_3O^-)_{O2}$ in (c) and (d) are normalized according to the peak maxima.

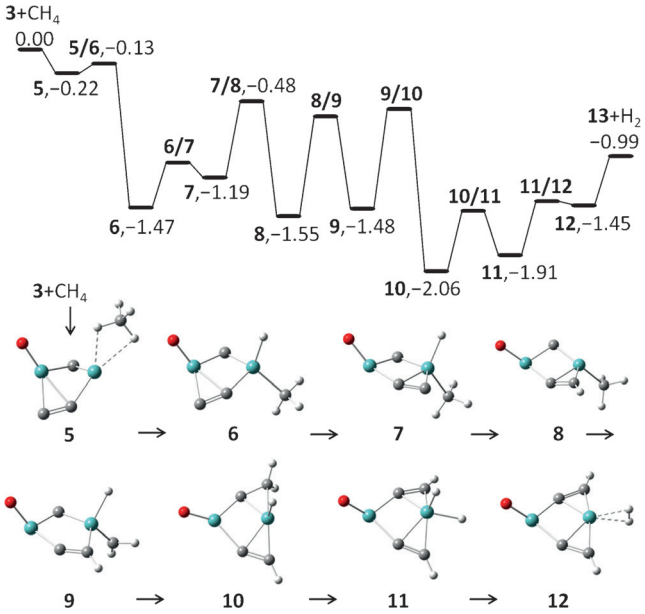

Figure 4. Reaction mechanism: DFT calculated potential energy profile for reaction of **3** with CH_4 in doublet spin state. The relative energies are in eV. The energies and structures of the transition states are listed in Figure S8.

$(Mo_2C_3O^-)_{CO}$. From the DFT calculated structures (Figure 3a), it is expected that isomer **2** is relatively more abundant in $(Mo_2C_3O^-)_{CO}$ and less abundant in $(Mo_2C_3O^-)_{O2}$, which is further supported by the PES experiments (Figure 3c). The combined information (MS/DFT/PES) concludes that the reactive component of $Mo_2C_3O^-$ is **3** while the unreactive component is **2**.

The reaction of **3** with CH_4 commences with formation of the encounter complex **5** with the binding energy of 0.22 eV (Figure 4). A Mo–CH_3 bond and a Mo–H bond are then formed through the OA mechanism by inserting the Mo atom into one C–H bond (**5**→**6**). The subsequent HAT processes (**7**→**8**→**9**) result in a metal carbene complex **9** ($MoCH_2$). After the C–C bond coupling (**9**→**10**), the reaction complex has enough energy (2.06 eV) to proceed the last HAT (from CH_2 to Mo), generating **11** with a six-fold coordinated Mo atom from which two H atoms can combine to form a H_2 unit (**11**→**12**). The dehydrogenation process finally completes (**12**→**13** + H_2). The energies of the reaction intermediates, transition states, and products are all lower than that of the separated reactants, so the DFT mechanism for **3** + CH_4 interprets the observed gas-phase reaction 2.

Investigations on the reactions of atomic clusters with CH_4 have revealed important mechanisms for methane activation.[5d–g,6,7] A key factor governing the cluster reactivity toward CH_4 is the spin density (SD) distribution. For the methane activation by extensively studied metal oxide clusters ($M_xO_y^{\pm}$), the SD on O atoms is very important: the localized and delocalized SD distributions correspond to high and low reactivity, respectively.[5f,g,15] It turns out that the SD on metal atoms well correlates with the reactivity of the molybdenum carbide clusters with methane herein. Both of the two-fold coordinated Mo (Mo_{2f}) atoms in **1** carry SD values of 0.70 μ_B while the Mo_{2f} of **3** has much less SD value (0.10 μ_B), which corresponds to positive (0.02 eV, Figure S9) and negative (−0.13 eV, Figure 4) overall barriers for C–H activation by **1** and **3**, respectively. This computational result interprets the experiments that the $Mo_2C_2^-$ (**1**) was unreactive ($\Phi < 0.01\,\%$) while $Mo_2C_3O^-$ (**3**) was reactive ($\Phi = 0.8\,\%$) with CH_4 (Figure 1). Moreover, the Mo_{2f} of **2** has a large SD value of 1.59 μ_B, which corresponds to a significant overall activation barrier (0.10 eV, Figure S9), in agreement with the structure characterization that **2** is the unreactive component of $Mo_2C_3O^-$ (Figures 2 and 3). It is noteworthy that the methane activation by Mo_{3f} atom (SD = −0.10 μ_B) of **2** has a negative overall-barrier (−0.05 eV, Figure S9) while the related dehydrogenation reaction is endothermic ($\Delta H_0 =$ 0.18 eV). It can be seen that the metal center (Mo) with *lower* SD is more favorable for methane activation through the OA mechanism, which is in contrast with the result that the oxygen center with *higher* SD is more favorable for methane activation through the HAT mechanism.[15] The lower SD of the metal center corresponds to more spin-paired electrons that are ready to be used for forming the σ bonds (M–C and M–H) in the OA process.[16] It can be concluded that the dissociative adsorption of CO onto $Mo_2C_2^-$ correctly manipulates the SD distribution on the metal centers and promotes the activation and transformation of methane.

CO is one of the most important ligands in coordination chemistry and organometallic chemistry.[17] The reactivity enhancement upon CO adsorption has been reported previously for gas phase ions. The bare Mn^- and Fe^- anions are inert with simple alkanes while the carbonyl complexes, $Mn(CO)_3^-$ [18] and $Fe(CO)_2^-$ [11a] are reactive. Bernhardt, Bonačić-Koutecký, and their co-workers have recently reported the cooperative coadsorption effects for the reac-

tions of Ru_n^+ clusters with CO and D_2.[19] Their experimental results indicated that the CO pre-adsorbed systems $Ru_4(CO)_{11}^+$ and $Ru_6(CO)_{14}^+$ can absorb up to seven and eight D atoms, respectively. In contrast, the bare Ru_4^+ and Ru_6^+ absorb only four and two D atoms, respectively. The experimental result of this study identified similar phenomenon of cooperative effect: in the reactions with CH_4, the $Mo_2C_2^-$ is inert while the CO pre-adsorbed $Mo_2C_3O^-$ can be reactive. It is noteworthy that the C–O units in the reported $Mn(CO)_3^-$, $Fe(CO)_2^-$, $Ru_4(CO)_{11}^+$, and $Ru_6(CO)_{14}^+$ ions are all un-broken. However, the $Mo_2C_3O^-$ isomer with unbroken C–O unit (**2** in Figure 3) is not reactive with CH_4. The reactive $Mo_2C_3O^-$ (**3**) is generated from CO dissociation, forming a C_2 unit and an oxo site which is not the active center with CH_4 (Figure S7). The CO dissociation and the large geometrical change properly tunes the SD distribution and results in the observed reactivity with methane.

In conclusion, thermal methane activation promoted by adsorption of CO on $Mo_2C_2^-$ cluster anions has been characterized by mass spectrometry, photoelectron spectroscopy, and density functional theory calculations. This study has identified a first example of noble-metal-free anions ($Mo_2C_3O^-$) that can react with methane through oxidative dehydrogenation under thermal collision conditions. The dissociative CO-adsorption tunes down the spin density distribution on one metal center, which then promotes methane activation through oxidative addition.

Experimental Section

The $Mo_xC_y^-$, $(Mo_2C_3O^-)_{CO}$, and $(Mo_2C_3O^-)_{O2}$ clusters were generated by laser ablation of a molybdenum metal disk compressed with isotope-enriched ^{98}Mo powder (99.45%, Trace Science International) in the presence of 0.5% CD_4, 0.5% CH_4/0.5% CO, and 0.5% CH_4/trace O_2 seeded in 5 atm He carrier gas. The clusters of interest were mass-selected by a quadrupole mass filter and entered into a linear ion trap reactor,[13] where they were confined and cooled by collisions with 4–6 Pa He gas for 0.9 ms and then interacted with CH_4, CD_4, or $^{13}CH_4$ for a period of time. The number of collisions (0.9 ms) between $Mo_2C_3O^-$ and He is around 1400, which can be high enough to thermalize the cluster.[20] Longer (> 1 ms) cooling time did not change the relative product intensity (Figure S4). The ions ejected from the ion trap were detected by a reflectron time-of-flight mass spectrometer.[13] The PES experiments were carried out with a separate instrument equipped with a laser ablation cluster source, a tandem time-of-flight mass spectrometer, and a photoelectron imaging spectrometer.[21] Briefly, the laser ablation generated cluster anions passed through two identical reflectors with Z-shaped configuration in the primary time-of-flight mass spectrometer and then the ions of interest were selected by a mass gate to interact with a wavelength-tunable laser beam delivered from an optical parametric oscillator based laser source (Continuum, Horizon). The kinetic energies (E_k) of the photo-detached electrons were measured by the photoelectron imaging spectrometer of which the energy resolution is better than 3% at E_k around 1.0 eV. The details of quantum chemistry calculations and Franck–Condon simulations are given in the Supporting Information, where a possible connection is postulated for this gas phase cluster chemistry and the condensed phase chemistry that addition of a few percent CO into methane feed promotes benzene formation over the Mo/HZSM-5 catalysts.[22]

Acknowledgements

This work is supported by the Chinese Academy of Sciences (Nos. XDA09030101 and YZ201318), the National Natural Science Foundation of China (Nos. 21325314, 21273247, 21290194, 21521062 and 21503015), and the Major Research Plan of China (No. 2013CB834603).

Keywords: density functional computations · mass spectrometry · methane activation · molybdenum carbides · photoelectron spectroscopy

How to cite: *Angew. Chem. Int. Ed.* **2016**, *55*, 5760–5764
Angew. Chem. **2016**, *128*, 5854–5858

[1] a) B. A. Arndtsen, R. G. Bergman, T. A. Mobley, T. H. Peterson, *Acc. Chem. Res.* **1995**, *28*, 154–162; b) T. V. Choudhary, E. Aksoylu, D. W. Goodman, *Catal. Rev. Sci. Eng.* **2003**, *45*, 151–203; c) G. A. Olah, *Angew. Chem. Int. Ed.* **2005**, *44*, 2636–2639; *Angew. Chem.* **2005**, *117*, 2692–2696.

[2] a) A. A. Fokin, P. R. Schreiner, *Chem. Rev.* **2002**, *102*, 1551–1593; b) M. Lersch, M. Tilset, *Chem. Rev.* **2005**, *105*, 2471–2526; c) R. Alizadeh, E. Jamshidi, G. P. Zhang, *J. Nat. Gas Chem.* **2009**, *18*, 124–130.

[3] a) R. A. Himes, K. D. Karlin, *Proc. Natl. Acad. Sci. USA* **2009**, *106*, 18877–18878; b) S. Scheller, M. Goenrich, R. Boecher, R. K. Thauer, B. Jaun, *Nature* **2010**, *465*, 606–609; c) X. Guo, G. Fang, G. Li, H. Ma, H. Fan, L. Yu, C. Ma, X. Wu, D. Deng, M. Wei, D. Tan, R. Si, S. Zhang, J. Li, L. Sun, Z. Tang, X. Pan, X. Bao, *Science* **2014**, *344*, 616–619; d) K. Kwapien, J. Paier, J. Sauer, M. Geske, U. Zavyalova, R. Horn, P. Schwach, A. Trunschke, R. Schlögl, *Angew. Chem. Int. Ed.* **2014**, *53*, 8774–8778; *Angew. Chem.* **2014**, *126*, 8919–8923; e) J. Gao, Y. Zheng, J.-M. Jehng, Y. Tang, I. E. Wachs, S. G. Podkolzin, *Science* **2015**, *348*, 686–690.

[4] a) M. Lin, A. Sen, *Nature* **1994**, *368*, 613–615; b) R. A. Periana, D. J. Taube, S. Gamble, H. Taube, T. Satoh, H. Fujii, *Science* **1998**, *280*, 560–564; c) A. Holmen, *Catal. Today* **2009**, *142*, 2–8; d) M. C. Alvarez-Galvan, N. Mota, M. Ojeda, S. Rojas, R. M. Navarro, J. L. G. Fierro, *Catal. Today* **2011**, *171*, 15–23.

[5] a) D. K. Böhme, H. Schwarz, *Angew. Chem. Int. Ed.* **2005**, *44*, 2336–2354; *Angew. Chem.* **2005**, *117*, 2388–2406; b) G. E. Johnson, R. Mitrić, V. Bonačić-Koutecký, A. W. Castleman, Jr., *Chem. Phys. Lett.* **2009**, *475*, 1–9; c) H.-J. Zhai, L.-S. Wang, *Chem. Phys. Lett.* **2010**, *500*, 185–195; d) J. Roithová, D. Schröder, *Chem. Rev.* **2010**, *110*, 1170–1211; e) S. M. Lang, T. M. Bernhardt, R. N. Barnett, U. Landman, *Angew. Chem. Int. Ed.* **2010**, *49*, 980–983; *Angew. Chem.* **2010**, *122*, 993–996; f) N. Dietl, M. Schlangen, H. Schwarz, *Angew. Chem. Int. Ed.* **2012**, *51*, 5544–5555; *Angew. Chem.* **2012**, *124*, 5638–5650; g) X.-L. Ding, X.-N. Wu, Y.-X. Zhao, S.-G. He, *Acc. Chem. Res.* **2012**, *45*, 382–390; h) S. Yin, E. R. Bernstein, *Int. J. Mass Spectrom.* **2012**, *321–322*, 49–65; i) K. R. Asmis, *Phys. Chem. Chem. Phys.* **2012**, *14*, 9270–9281; j) D. J. Harding, C. Kerpal, G. Meijer, A. Fielicke, *Angew. Chem. Int. Ed.* **2012**, *51*, 817–819; *Angew. Chem.* **2012**, *124*, 842–845; k) R. A. J. O'Hair, *Int. J. Mass Spectrom.* **2015**, *377*, 121–129; l) H. Schwarz, *Angew. Chem. Int. Ed.* **2015**, *54*, 10090–10100; *Angew. Chem.* **2015**, *127*, 10228–10239.

[6] P. B. Armentrout, J. L. Beauchamp, *Acc. Chem. Res.* **1989**, *22*, 315–321.

[7] H. Schwarz, *Isr. J. Chem.* **2014**, *54*, 1413–1431.

[8] a) U. Achatz, C. Berg, S. Joos, B. S. Fox, M. K. Beyer, G. Niedner-Schatteburg, V. E. Bondybey, *Chem. Phys. Lett.* **2000**, *320*, 53–58; b) C. Adlhart, E. Uggerud, *Chem. Commun.* **2006**,

2581 – 2582; c) Y.-X. Zhao, Z.-Y. Li, Z. Yuan, X.-N. Li, S.-G. He, *Angew. Chem. Int. Ed.* **2014**, *53*, 9482 – 9486; *Angew. Chem.* **2014**, *126*, 9636 – 9640.
[9] C. P. G. Butcher, A. Dinca, P. J. Dyson, B. F. G. Johnson, P. R. R. Langridge-Smith, J. S. McIndoe, *Angew. Chem. Int. Ed.* **2003**, *42*, 5752 – 5755; *Angew. Chem.* **2003**, *115*, 5930 – 5933.
[10] J.-H. Meng, X.-J. Deng, Z.-Y. Li, S.-G. He, W.-J. Zheng, *Chem. Eur. J.* **2014**, *20*, 5580 – 5583.
[11] a) R. N. McDonald, D. J. Reed, A. K. Chowdhury, *Organometallics* **1989**, *8*, 1122 – 1124; b) H.-F. Li, Z.-Y. Li, Q.-Y. Liu, X.-N. Li, Y.-X. Zhao, S.-G. He, *J. Phys. Chem. Lett.* **2015**, *6*, 2287 – 2291.
[12] a) L.-S. Wang, L.-X. Tao, M.-S. Xie, G.-G. Xu, J.-S. Huang, Y.-D. Xu, *Catal. Lett.* **1993**, *21*, 35 – 41; b) J. Shu, A. Adnot, B. P. A. Grandjean, *Ind. Eng. Chem. Res.* **1999**, *38*, 3860 – 3867; c) H. Zheng, D. Ma, X. Bao, J. Z. Hu, J. H. Kwak, Y. Wang, C. H. F. Peden, *J. Am. Chem. Soc.* **2008**, *130*, 3722 – 3723; d) D. Zhou, S. Zuo, S. Xing, *J. Phys. Chem. C* **2012**, *116*, 4060 – 4070.
[13] Z. Yuan, Z.-Y. Li, Z.-X. Zhou, Q.-Y. Liu, Y.-X. Zhao, S.-G. He, *J. Phys. Chem. C* **2014**, *118*, 14967 – 14976.
[14] G. Kummerlöwe, M. K. Beyer, *Int. J. Mass Spectrom.* **2005**, *244*, 84 – 90.
[15] a) X.-N. Wu, Y.-X. Zhao, W. Xue, Z.-C. Wang, S.-G. He, X.-L. Ding, *Phys. Chem. Chem. Phys.* **2010**, *12*, 3984 – 3997; b) J.-H. Meng, Y.-X. Zhao, S.-G. He, *J. Phys. Chem. C* **2013**, *117*, 17548 – 17556.
[16] a) X.-G. Zhang, R. Liyanage, P. B. Armentrout, *J. Am. Chem. Soc.* **2001**, *123*, 5563 – 5575; b) R. Georgiadis, P. B. Armentrout, *J. Phys. Chem.* **1988**, *92*, 7067 – 7074; c) R. Georgiadis, P. B. Armentrout, *Int. J. Mass Spectrom. Ion Processes* **1989**, *89*, 227 – 247; d) R. Z. Hinrichs, P. A. Willis, H. U. Stauffer, J. J. Schroden, H. F. Davis, *J. Chem. Phys.* **2000**, *112*, 4634 – 4643.
[17] Q.-Y. Liu, S.-G. He, *Chem. J. Chin. U.* **2014**, *35*, 665 – 688.
[18] R. N. McDonald, M. T. Jones, *J. Am. Chem. Soc.* **1986**, *108*, 8097 – 8098.
[19] S. M. Lang, T. M. Bernhardt, M. Krstić, V. Bonačić-Koutecký, *Angew. Chem. Int. Ed.* **2014**, *53*, 5467 – 5471; *Angew. Chem.* **2014**, *126*, 5571 – 5575.
[20] T. M. Bernhardt, *Int. J. Mass Spectrom.* **2005**, *243*, 1 – 29.
[21] Q.-Y. Liu, L. Hu, Z.-Y. Li, C.-G. Ning, J.-B. Ma, H. Chen, S.-G. He, *J. Chem. Phys.* **2015**, *142*, 164301.
[22] R. Ohnishi, S. Liu, Q. Dong, L. Wang, M. Ichikawa, *J. Catal.* **1999**, *182*, 92 – 103.

Received: January 20, 2016
Published online: April 6, 2016

